THE STUDY OF MONOTONICITY OF AUSM-TYPE SCHEMES IN SHOCK DISCONTINUITIES

Kyu Hong Kim[2], Chongam Kim[1], Oh-Hyun Rho[1] and Kyung-Tae Lee[2]
[1] Department of Aerospace Engineering,
Seoul National University, 151-742, Seoul, Korea
[2] Sejong-Lockheed Martin Aerospace Research Center,
Sejong University, 143-747, Seoul, Korea

Keywords: *AUSMPW+, Shock discontinuity, Monotonic characteristic, Oscillation, Sonic transition position*

Abstract

AUSM-type schemes share the advection property. Since it always transfers information like hyperbolic equation, the advection property is not appropriate in applied to subsonic flows which are governed by elliptic PDE. The disagreement between the advection property and physical phenomena induces excessive or insufficient fluxes behind shocks where the flow is subsonic and eventually shows oscillatory behaviors. In order to settle this disadvantage, a scheme should calculate fluxes behind a shock discontinuity with the consideration of physical phenomena as accurately as possible.

AUSMPW+ is modified to capture a shock wave exactly with monotonic characteristic in considering physical phenomena accurately as possible and whether a cell-interface of shock region is in a subsonic or a supersonic region. In addition, it could capture shocks robustly independent to grid system.

1 Introduction

AUSM-type schemes are developed combining the accuracy of FDS and the robustness of FVS. The first AUSM type scheme, AUSM [1] is simple as FVS but accurate since the information of both side properties could be exchanged across a cell-interface. Accuracy was improved in only boundary or shear layers. However, it has been still shown dissipative results in capturing a shock. Moreover, the advection property causes a monotonic problem. AUSM had the both of accuracy and monotonic characteristic problem in capturing shocks, though there is a noticeable enhancement of accuracy in only boundary layers. In order to improve the accuracy problem, AUSM+ [2] was developed with the definition of the speed of sound at a cell interface which could give the information on a sonic transition position. So AUSM+ can capture a shock exactly if a sonic transition position is on a cell-interface. However, in condition that a sonic transition position is deviated from a cell-interface, the monotonic characteristic cannot be maintained any longer. In order to improve the monotonic characteristic, AUSMPW [3] and AUSMPW+ [4,5] were developed. They control the advection property using pressure based weight functions and remove oscillations in a shock region successfully. But in some grid systems, they still show oscillations though it is much less than that in AUSM or AUSM+. It is due to the advection property which is not suitable to physical phenomena.

In this paper, AUSMPW+ is modified by newly defined speed of sound. It can remove oscillations completely independent to grid systems and represent physical phenomena accurately. The modified AUSMPW+ is called M-AUSMPW+ temporally for convenience.

2 Governing Equation

The two dimensional Euler equation as conservative form is as follows.

$$\frac{\partial \boldsymbol{Q}}{\partial t}+\frac{\partial \boldsymbol{E}}{\partial x}+\frac{\partial \boldsymbol{F}}{\partial y}=0, \qquad (1)$$

and flow and flux vectors are written as

$$\boldsymbol{Q}=\begin{pmatrix}\rho\\ \rho u\\ \rho v\\ \rho e_t\end{pmatrix}, \mathbf{E}=\begin{pmatrix}\rho u\\ \rho u^2+p\\ \rho uv\\ (\rho e_t+p)u\end{pmatrix}, \mathbf{F}=\begin{pmatrix}\rho v\\ \rho vu\\ \rho v^2+p\\ (\rho e_t+p)v\end{pmatrix}, \qquad (2)$$

where e_t is total internal energy.

For calorically perfect gas the equation of state is given by

$$p=(\gamma-1)\rho e=(\gamma-1)\rho\left(e_t-\frac{1}{2}\left(u^2+v^2\right)\right), \qquad (3)$$

with $\gamma=1.4$ for air.

3 Spatial Discretization

The flux which is constructed by AUSM-type schemes is written as follows.

$$\mathbf{F}_{\frac{1}{2}}=\overline{M}_L^{+}c_{\frac{1}{2}}\boldsymbol{\Phi}_L+\overline{M}_R^{-}c_{\frac{1}{2}}\boldsymbol{\Phi}_R+\left(\mathrm{P}_L^{+}\mathbf{P}_L+\mathrm{P}_R^{-}\mathbf{P}_R\right), \qquad (4)$$

where $\boldsymbol{\Phi}=(\rho,\rho u,\rho H)^T$ and $\boldsymbol{P}=(0,p,0)^T$.

The Mach number and pressure splitting functions of M-AUSMPW+ are the same as those of AUSMPW+ [4] and pressure based weight functions $f_{L,R}$ and w are also the same.

Only the difference from AUSMPW+ is the speed of sound at cell-interfaces. The problematic mach number region where AUSMPW+ shows the oscillatory behavior is $0<M_L^*M_R^*<1$. Thus the speed of sound in M-AUSMPW+ is modified only in this region.

i) $\left|M_L^*\right|>1,\ \left|M_R^*\right|<1,\ 0<M_L^*M_R^*<1, \qquad (5)$

$$c_{\frac{1}{2}}=-\left(u_R-2\frac{\rho_L}{\rho_R}u_L\right)+\sqrt{\left(u_R-2\frac{\rho_L}{\rho_R}u_L\right)^2-u_R^{\,2}},$$

$$P_R^{-}=1-\frac{\rho_L u_L(u_L-u_R)+p_L}{p_R}.$$

ii) $\left|M_R^*\right|>1,\ \left|M_L^*\right|<1,\ 0<M_L^*M_R^*<1, \qquad (6)$

$$c_{\frac{1}{2}}=-\left(u_L-2\frac{\rho_R}{\rho_L}u_R\right)+\sqrt{\left(u_L-2\frac{\rho_R}{\rho_L}u_R\right)^2-u_L^{\,2}},$$

$$P_L^{-}=1-\frac{\rho_R u_R(u_R-u_L)+p_R}{p_L}.$$

iii) elsewhere (7)

- $\frac{1}{2}(U_L+U_R)>0:\ c_{\frac{1}{2}}=c^{*2}/\max(|U_L|,c^*)$
- $\frac{1}{2}(U_L+U_R)<0:\ c_{\frac{1}{2}}=c^{*2}/\max(|U_R|,c^*)$.

Superscript * indicate the property at the sonic speed.

4 Analysis of Oscillatory Behaviors in Shock regions

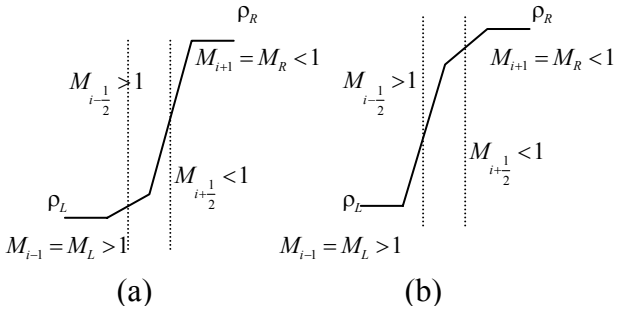

Fig. 1. Schematics of two types of shock capturing along the sonic transition position.

Figure 1 shows the schematics of numerical shock structure. In case of (a) the sonic transition position is located between ith and i+1th cell center points. Since $M_L^*M_R^*=1$, the Mach number at the cell-interface $i+1/2$, $M_{i+\frac{1}{2}}=M_i^*M_{i+1}^*$, is always smaller than one. It means that a sonic transition position, where $M_L^*M_R^*=1$, is located on the left of the cell-interface $i+1/2$. The case (b) is that the sonic transition position is located between i-1th and ith cell center points. The Mach number at the cell-interface $i-1/2$, $M_{i-\frac{1}{2}}=M_{i-1}^*M_i^*$, is always greater than one. It means that the sonic transition position is located on the right of cell-interface $i-1/2$.

Now, the characteristic of FVS type schemes and AUSM-type schemes will be studied in each case respectively.

Since van Leer scheme [6] transfers a flux according to the sign of eigenvalue, physical phenomena could be considered somewhat accurately. However there is no way to know where a sonic transition position is located, i.e., van Leer scheme cannot distinguish between Fig. 1(a) and Fig. 1(b). Thus even if a sonic transition position is located right on a cell-interface, van Leer scheme produces much different fluxes compared to physical fluxes. All of these errors act as numerical dissipation and accuracy gets worse.

AUSM+ improved accuracy. Since the speed of sound in AUSM+ uses Prandtl relation of stationary normal shock, AUSM+ can recognize where a sonic transition position is, i.e., AUSM+ can distinguish between Fig. 1(a) and Fig. 1(b). As a result, AUSM+ can capture a shock discontinuity exactly without oscillations providing that a sonic transition position is located on a cell-interface. However, the advection property of AUSM+ makes oscillatory problems if a sonic transition position is located out of a cell-interface. Behind a shock discontinuity a flow is governed by elliptic equations, on the other hand, AUSM+ always maintain hyperbolic equations because of the advection property. In non shock-aligned grid system, this is the pivotal reason of oscillation.

AUSMPW+ is designed to remove numerical oscillation shown in AUSM+ and improve accuracy in capturing the oblique shock. The oscillation in AUSM+ is due to the insufficient numerical dissipation caused by the advection property in subsonic flow region. The basic idea of AUSMPW+ is the control of advection property by the pressure based weight function and the production of proper numerical dissipation.

In case of Fig.2(a), the mass flux of van Leer scheme, which does not show oscillation phenomena, is as follows.

Van leer : $F = u_L \rho_L + M_R^- c_R \rho_R$.

AUSM+ : $F = u_L \rho_L + M_R^- c_{\frac{1}{2}} \rho_L$.

AUSMPW+:

$$F = u_L \rho_L + M_R^- c_{\frac{1}{2}} \rho_L + M_R^- c_{\frac{1}{2}} \left[w(1+f_R)(\rho_R - \rho_L) + \frac{p_R - p_L}{p_s} \right].$$

Terms of M^- of AUSMPW+, AUSM+ and van Leer FVS are fluxes transferred to the opposite direction compared to a flow direction. The term of M^- of AUSM+ is much smaller than that of van Leer or AUSMPW+ scheme because of the advection property. So the total flux of AUSM+ at a cell-interface is transferred to a flow direction excessively by the ratio of density and speed of sound. If solutions are converged, after all, the numerical oscillation is generated. AUSMPW+ decreases fluxes by adding the terms of pressure based weight function f and w. It can remove most of oscillations, however, AUSMPW+ shows a little numerical oscillation as in Fig. 7.

In case M_i goes to M_L asymptotically, the physical flux is $F = u_L \rho_L$, since the cell-interface is located on the supersonic region. The flux of van Leer still includes the term of M^- and the total flux becomes smaller than the physical flux. After a solution is converged, van Leer scheme capture shock discontinuity through two intermediate cells even in a shock-aligned grid system as the case (a) in Fig.7. On the other hand, in case of AUSM+ and AUSMPW+, $M_{R,i+1/2}$ goes to one and M_R^- becomes zero. The total flux at a cell-interface is exactly the same as the physical flux. AUSM+ and AUSMPW+ could represent physical shock phenomena exactly and capture shock accurately without numerical oscillations as the case (a) in Fig.7.

In Fig. 2(b), since the flow is supersonic at a cell-interface, the exact physical flux is $F = u_L \rho_L$. The mass flux of AUSM+ and AUSMPW+ is also $F = u_L \rho_L$. There seems to be no problem. However, AUSM+ also shows numerical oscillations because of the advection

property. The main reason is the excessive flux at the next cell-interface $i+1/2$ compared with those of van Leer scheme and AUSMPW+. The mass flux of van Leer scheme which does not show oscillation phenomena, is in the cell-interface $i+1/2$ as follows.

Van leer : $F = M_L^+ c_L \rho_L + M_R^- c_R \rho_R$.

AUSM+ : $F = M_L^+ c_{\frac{1}{2}} \rho_L + M_R^- c_{\frac{1}{2}} \rho_L$.

AUSMPW+ :

$$F = M_L^+ c_{\frac{1}{2}} \rho_L + M_R^- c_{\frac{1}{2}} \rho_L + M_R^- c_{\frac{1}{2}} \left[w(1+f_R)(\rho_R - \rho_L) + \frac{p_R - p_L}{p_s} \right].$$

AUSMPW+ reduces fluxes by adding the terms of pressure based weight function f and w, and as a result, it does not show numerical oscillations like van Leer FVS. If M_i goes to M_R asymptotically, AUSMPW+ transfers the same flux as the physical flux, $F = u_L \rho_L$. It is possible to capture shocks exactly without numerical oscillations as the case (e) in Fig. 7. Even in $M_R < M_i < 1$, by thanks to the term of pressure based weight function, f and w, AUSMPW+ can transfer an appropriate flux across a cell-interface and never show numerical oscillations.

Based on analyzing above results, to remove the oscillations completely throughout a whole Mach number region, the proper numerical dissipation seems to be required in the problematic region , $|M_L^*| > 1$, $|M_R^*| < 1$, $0 < M_L^* M_R^* < 1$ where a shock is captured as in Fig. 1(a). Governing equations in this region are as follows.

Continuity equation:

$$\rho_L u_L = \rho_i u_i + \rho_R M_R^- c = \rho_i u_i - \rho_R 0.25 \left(1 - \frac{u_R}{c}\right)^2 c = \rho_R u_R \quad . \qquad (8)$$

Momentum equation:

$$\rho_L u_L^{\,2} + p_L = \rho_i u_i^{\,2} + p_i + \rho_R M_R^- c\, u_R + P_R^- p_R = \rho_R u_R^{\,2} + p_R \quad . \qquad (9)$$

If Eqs. (8) and (9) satisfy the condition of Fig. 1(a) and the expansion shock solution is excluded, the following equation is simplified as follows.

When $|M_L^*| > 1$, $|M_R^*| < 1$, $0 < M_L^* M_R^* < 1$, (5)

$$c_{\frac{1}{2}} = -\left(u_R - 2\frac{\rho_L}{\rho_R} u_L\right) + \sqrt{\left(u_R - 2\frac{\rho_L}{\rho_R} u_L\right)^2 - u_R^{\,2}} \quad ,$$

$$P_R^- = 1 - \frac{\rho_L u_L (u_L - u_R) + p_L}{p_R} \quad .$$

With the $c_{\frac{1}{2}}$ and P_R^-, M-AUSMPW+ could remove the numerical oscillation completely.

The monotonic characteristic of van Leer, AUSM+, AUSMPW+, and M-AUSMPW+ can be summarized as follows. Van Leer scheme always maintains the monotonic characteristic. As mentioned above, since it cannot distinguish from Fig. 1(a) and Fig. 1(b), it show the inaccurate discontinuity. AUSM+ always shows oscillation, especially, in $1 < M_i < M_L$ oscillations are more severe. AUSMPW+ removes oscillation successfully even though it shows a little oscillation in $1 < M_i < M_L$. At last, M-AUSMPW+ never show numerical oscillation in any case, moreover, it can capture shocks with only one intermediate cell.

Table 1. the comparison of a monotonic characteristic of each scheme (case1: $M_i = M_L$; case 2: $1 < M_i < M_L$; case 3: $M_R < M_i < 1$; case4: $M_i = M_R$)

	case 1	case 2	case 3	case4
Van Leer	mono	mono	mono	mono
AUSM+	mono	oscil	oscil	mono
AUSMPW+	mono	oscil	mono	mono
M-AUSMPW+	mono	mono	mono	mono

5 Analysis of the Monotonic Characteristic of AUSM-type schemes

The inveterate problem of AUSM-type schemes, i.e., oscillatory problems induced by a shock discontinuity, will be analyzed. The monotonic characteristic of each scheme will be proven based on numeric and mathematics.

Figure 2 is a schematic of a numerical shock structure in computations.

If a solution would be converged completely, fluxes of all cell-interfaces are the same and expressed by

$$\boldsymbol{F}_L = \boldsymbol{F}_1 = \boldsymbol{F}_2 = \boldsymbol{F}_3 = \boldsymbol{F}_R \qquad (10)$$

At this point, to maintain the monotonic characteristic, following conditions should be satisfied.

Density condition:

$$\rho_L \le \rho_1 \le \rho_2 \le \rho_3 \le \rho_R \qquad (11)$$

pressure condition:

$$p_L \le p_1 \le p_2 \le p_3 \le p_R \qquad (12)$$

Mach number condition:

$$M_L \ge M_1 \ge M_2 \ge M_3 \ge M_R \qquad (13)$$

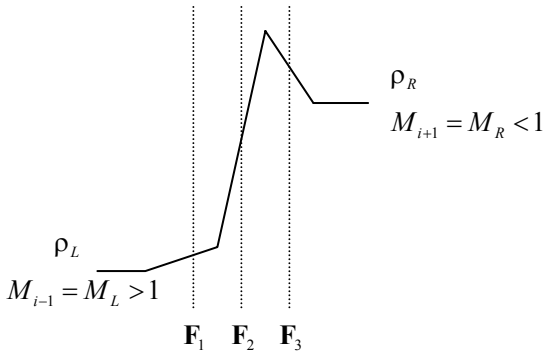

Fig. 2. The schematic of numerical shock discontinuity.

At first, if the converged solution satisfies Mach number condition of Eq.(13), the critical Mach number also satisfy Eq.(14) since critical Mach number show the same tendency as physical Mach number

$$M_L^* \ge M_1^* \ge M_2^* \ge M_3^* \ge M_R^* \qquad (14)$$

Since the solution is assumed to be converged completely, mass fluxes at each cell-interface are the same as follows.

$$\begin{aligned}\rho_L u_L &= \rho_L \overline{M}_L^+ + \rho_1 \overline{M}_1^- = \rho_1 \overline{M}_1^+ + \rho_2 \overline{M}_2^- \\ &= \rho_2 \overline{M}_2^+ + \rho_3 \overline{M}_3^- = \rho_3 \overline{M}_3^+ + \rho_R \overline{M}_R^- \\ &= \rho_R u_R\end{aligned} \qquad (15)$$

In AUSM-type scheme or van Leer scheme, $\dfrac{\overline{M}_R^+}{\overline{M}_3^+} < 1$ from Eq. (14).

Then, $\rho_3 = \rho_R \dfrac{\overline{M}_R^+}{\overline{M}_3^+} < \rho_R$, $\rho_3 < \rho_R$ (16)

$$\rho_2 < \rho_3 \frac{\overline{M}_3^+}{\overline{M}_2^+} < \rho_3 \qquad (17)$$

with the same way,

$$\rho_L \le \rho_1 \le \rho_2 \le \rho_3 \le \rho_R \qquad (18)$$

In case of pressure condition, converged pressures at each cell can be determined by the equation of state.

$$p = \rho \frac{\gamma - 1}{2\gamma}\left[2H - \left(M^* c^*\right)^2\right]. \qquad (19)$$

and the pressure condition of Eq. (20) is also satisfied.

$$p_L \le p_1 \le p_2 \le p_3 \le p_R \qquad (20)$$

Therefore, in FVS or AUSM-type scheme, what the Mach number distribution satisfies Eq.(14) means that all distributions of property are monotonic, i.e., only if the distribution of Mach number is monotonic through a shock discontinuity, it is allowable to say that the scheme capture shocks with the monotonic characteristic.

Coming back to Eq.(15), the last equation is not used yet. From the last equation, the following condition is introduced.

$$\rho_L \overline{M}_L^- = 0 = \rho_1 \overline{M}_1^- \rightarrow \overline{M}_1^- = 0 \qquad (21)$$

Equation (21) is the necessary condition for the monotonic capturing with only one intermediate cell. In order to satisfy Eq. (21), the Mach number of cell 1 should be greater than one and less than M_L or the Mach number splitting function $\overline{M}_1^-$ should be zero itself.

Van Leer scheme does not satisfy Eq.(21). So, it captures shocks with two intermediate cells as shown in Fig. 7.

Fluxes of AUSM-type schemes may be written as follows

$$\begin{aligned}
\boldsymbol{F}_L &= U_L\boldsymbol{\Phi}_L + \boldsymbol{p}_L \\
\boldsymbol{F}_1 &= \overline{M}_{LL}c_{LL}\boldsymbol{\Phi}_L + \overline{M}^-_{1R}c_{1R}\boldsymbol{\Phi}_1 + \boldsymbol{p}_L + P^-_{1R}\boldsymbol{p}_1 \\
\boldsymbol{F}_2 &= \overline{M}^+_{1L}c_{1L}\boldsymbol{\Phi}_1 + \overline{M}^-_{2R}c_{2R}\boldsymbol{\Phi}_2 + P^+_{1L}\boldsymbol{p}_1 + P^-_{2R}\boldsymbol{p}_2 \\
\boldsymbol{F}_3 &= \overline{M}^+_{2L}c_{2L}\boldsymbol{\Phi}_2 + \overline{M}^-_{RR}c_{RR}\boldsymbol{\Phi}_R + P^+_{2L}\boldsymbol{p}_2 + P^-_{RR}\boldsymbol{p}_R \\
\boldsymbol{F}_R &= U_R\boldsymbol{\Phi}_R + \boldsymbol{p}_R
\end{aligned} \tag{22}$$

If there exists converged solutions and converged solutions were obtained after computations, fluxes at all of cell-interfaces are the same.

i) $\boldsymbol{F}_1 = \boldsymbol{F}_2$

mass flux :

$$\begin{aligned}
&\rho_1\left(\overline{M}^+_{1L}c_{1L} - \overline{M}^-_{1R}c_{1R}\right) \\
&+ \rho_2\overline{M}^-_{2R}c_{2R} - \rho_L M_{LL}c_{LL} = 0
\end{aligned} \tag{23}$$

momentum flux :

$$\begin{aligned}
f_{12} &= \rho_1 M^*_1 c^*\left(\overline{M}^+_{1L}c_{1L} - \overline{M}^-_{1R}c_{1R}\right) \\
&+ \rho_2 M^*_2 c^*\overline{M}^-_{2R}c_{2R} - \rho_L M^*_L c^* M_{LL}c_{LL} \\
&+ p_1\left(P^+_{1L} - P^-_{1R}\right) + p_2 P^-_{2R} - p_L = 0
\end{aligned} \tag{24}$$

energy flux:

$$\begin{aligned}
&\rho_1 H_1\left(\overline{M}^+_{1L}c_{1L} - \overline{M}^-_{1R}c_{1R}\right) \\
&+ \rho_2 H_2\overline{M}^-_{2R}c_{2R} - \rho_L H_L M_{LL}c_{LL} = 0
\end{aligned} \tag{25}$$

ii) $\boldsymbol{F}_2 = \boldsymbol{F}_3$

mass flux :

$$\begin{aligned}
&\rho_2\left(\overline{M}^+_{2L}c_{2L} - \overline{M}^-_{2R}c_{2R}\right) \\
&+ \rho_R\overline{M}^-_{RR}c_{RR} - \rho_1\overline{M}^+_{1L}c_{1L} = 0
\end{aligned} \tag{26}$$

momentum flux :

$$\begin{aligned}
f_{23} &= \rho_2 M^*_2 c^*\left(\overline{M}^+_{2L}c_{2L} - \overline{M}^-_{2R}c_{1R}\right) \\
&+ \rho_R M^*_R c^*\overline{M}^-_{RR}c_{RR} - \rho_1 M^*_1 c^*\overline{M}^+_{1L}c_{1L} \\
&+ p_2\left(P^+_{2L} - P^-_{2R}\right) + p_R P^-_{RR} - p_1 P^+_{1L} = 0
\end{aligned} \tag{27}$$

energy flux:

$$\begin{aligned}
&\rho_2 H_2\left(\overline{M}^+_{2L}c_{2L} - \overline{M}^-_{2R}c_{2R}\right) \\
&+ \rho_R H_R\overline{M}^-_{RR}c_{RR} - \rho_1 H_1\overline{M}^+_{1L}c_{1L} = 0
\end{aligned} \tag{28}$$

After simplify Eqs.(23) to (28), it is easily known that the function f_{12} and f_{23} of Eq.(24) and Eq.(27) are the functions of velocity of cell 2 with the parameter of velocity of cell 1, i.e.,

$$f_{12} = f_{12}(U_2) = 0,\ f_{23} = f_{23}(U_2) = 0. \tag{29}$$

If there are the velocity of cell 2 which satisfies Eq.(28), there exists the solution which shows monotonic distributions of Mach number, density and pressure.

Figure 3 is the results for AUSM+. If the triple intersection point of functions f_{12}, f_{23} and zero exists, i.e., the solution of equations $f_{12} = f_{12}(U_2) = 0$ and $f_{23} = f_{23}(U_2) = 0$ exists. If the triple point exists and Mach number of cell 2 is less than M_R, it means that the Mach number distribution does not satisfy monotonic Mach number condition of Eq. (14). On the other hand, if the triple point exists and Mach number of cell 2 is greater than M_R, the Mach number distribution does satisfy monotonic Mach number condition and all property through a shock discontinuity has monotonic distributions.

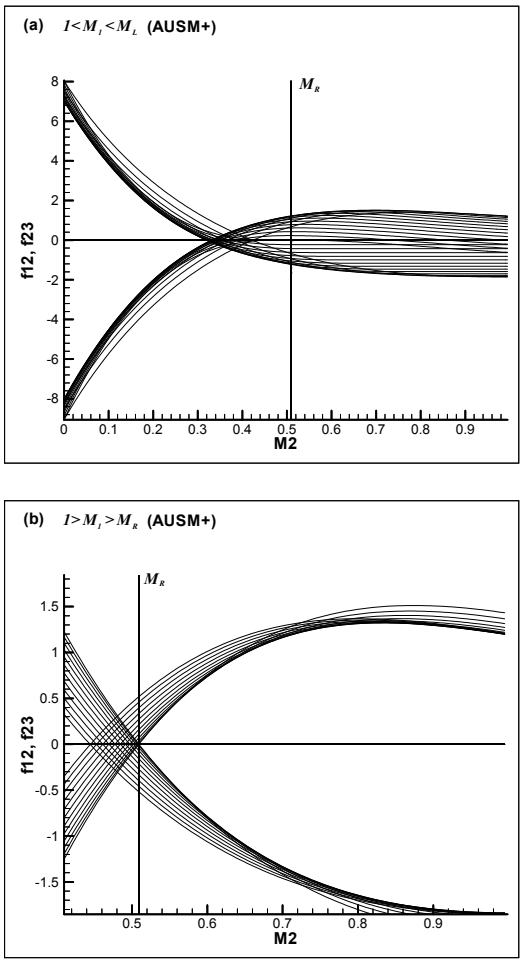

Fig. 3. f_{12} and f_{23} of AUSM+.

Form Fig. 3, AUSM+ always shows numerical oscillation. Especially, when

$1 < M_1 < M_L$, the converged solution is predicted to show severe oscillatory behaviors.

In Fig. 4, when $1 < M_1 < M_L$, M_2 is less than M_R in some region. It means that AUSMPW+ does not satisfy monotonic conditions and shows oscillations. However, since M_2 is slightly less than M_R, oscillations are so small that there is a slight problem in real applications. In contrast, when $1 > M_1 > M_R$, M_2 is always greater than M_R and the monotonic converged solution could be obtained.

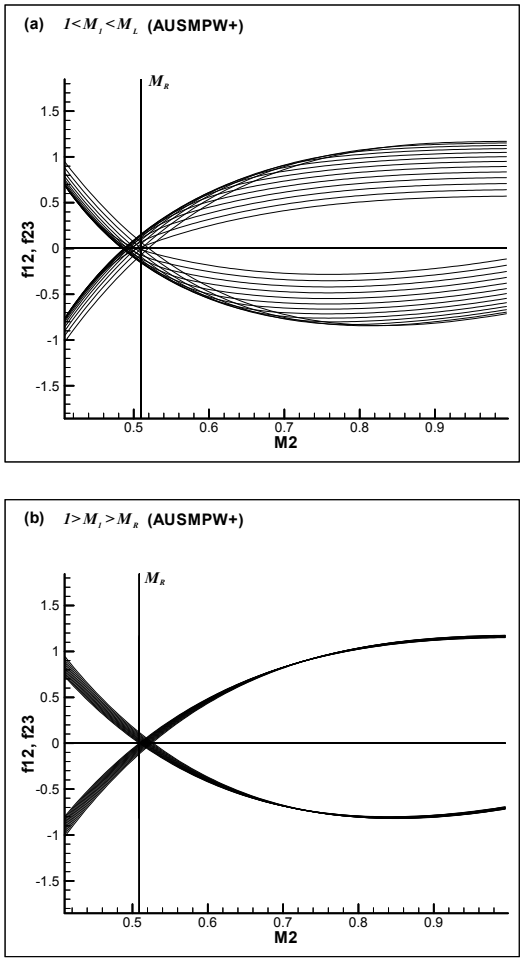

Fig. 4. f_{12} and f_{23} of AUSMPW+.

Figure 5(a) and 5(b) show that M_2 is always greater than M_R . It means that the solution by M-AUSMPW+ always shows the monotonic characteristic.

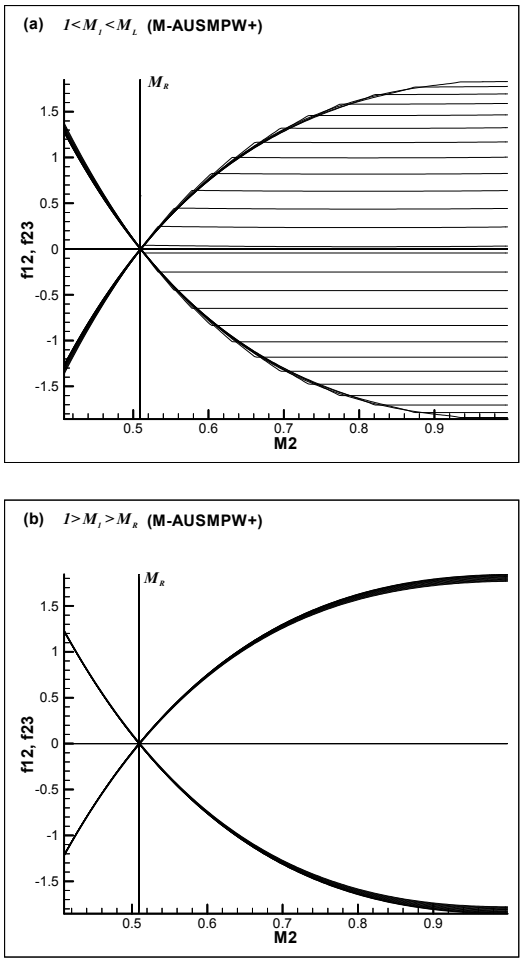

Fig. 5. f_{12} and f_{23} of M-AUSMPW+.

6 Result

6.1 Characteristic of shock-capturing according to a sonic transition position

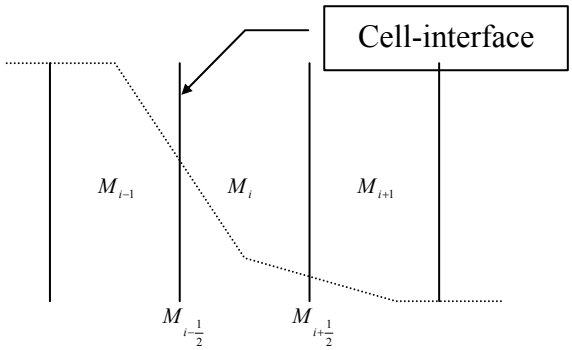

Fig. 6. Definition of indexes of cells and cell-interfaces.

Following numerical tests are performed to investigate the shock-capturing characteristic of each scheme according to a sonic transition position and a cell-interface. The Mach number at the cell-interface $i+1/2$ is $M_{i+\frac{1}{2}} = M_i^* M_{i+1}^*$.

The initial conditions of each case are as follows

When $M_L > 1 > M_R$

Case (a) : $M_{i-1} = M_i = M_L$, $M_{i+1} = M_R$, $M_{i-\frac{1}{2}} = M_L$, $M_{i+\frac{1}{2}} = 1$

Case (b) : $M_{i-1} = M_L$, $M_i = 0.5(M_L + 1)$, $M_{i+1} = M_R$, $M_{i-\frac{1}{2}} > 1$, $M_{i+\frac{1}{2}} < 1$

Case (c) : $M_{i-1} = M_L$, $M_i = 1$, $M_{i+1} = M_R$, $M_{i-\frac{1}{2}} > 1$, $M_{i+\frac{1}{2}} < 1$

Case (d) : $M_{i-1} = M_L$, $M_i = 0.5(M_R + 1)$, $M_{i+1} = M_R$, $M_{i-\frac{1}{2}} > 1$, $M_{i+\frac{1}{2}} > 1$

Case (e) : $M_{i-1} = M_L$, $M_i = M_{i+1} = M_R$, $M_{i-\frac{1}{2}} = 1$, $M_{i+\frac{1}{2}} = M_R$

Figure 7 shows the pressure distributions of each scheme according to each initial condition.

As mentioned above, though it shows the monotonic characteristic in capturing shocks, van Leer scheme captures shocks through two intermediate cells even if sonic transition position is located on a cell-interface like cases (a) and (e).

AUSM+ always maintains the hyperbolic characteristics even in a subsonic region because of the advection property. Since hyperbolic characteristic is exactly coincident with cases (a) and (e), AUSM+ does not show oscillations. The rest of cases, however, show oscillations, since the advection property is not appropriate to solve a subsonic region.

AUSMPW+ can capture shock exactly maintaining the advection property in cases (a) and (e) which a sonic transition position is located on a cell-interface. If the sonic transition position is deviated from a cell-interface, AUSMPW+ controls the advection property appropriately using pressure weighted function f and w, and as a result, removes the oscillations. However, in case (b), even AUSMPW+ shows small oscillation. It is caused by the fact that, as sonic transition position approach a cell-interface, the speed of sound of AUSMPW+ reduces the numerical dissipation so rapidly that it induces the numerical oscillations. Lastly, M-AUSMPW+ shows the best results and they are with the same level of accuracy. Shocks are captured through only one or no intermediate cell in all cases.

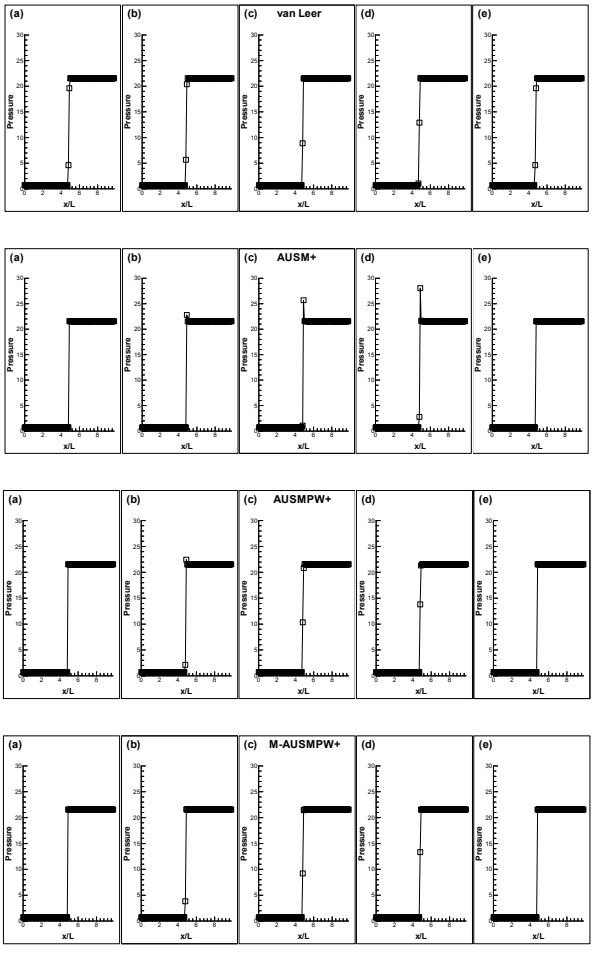

Fig. 7. Comparison of pressure distribution of each scheme along the Mach number at cell i.

6.2 Hypersonic flow around a cut cylinder

In case of a strong shock like a hypersonic flow problem, there may occur many accuracy or robustness problems according to the

distance between a sonic transition position and a cell-interface. For example, in non shock-aligned grid system, large numerical errors are induced across shocks, propagate downstream along flows and have bad influences on accuracy.[5] Aligning shocks with grid system for the improvement of accuracy could give the ability to capture shock without numerical dissipation. However, it is liable that insufficient numerical dissipation magnifies numerical shock instability.

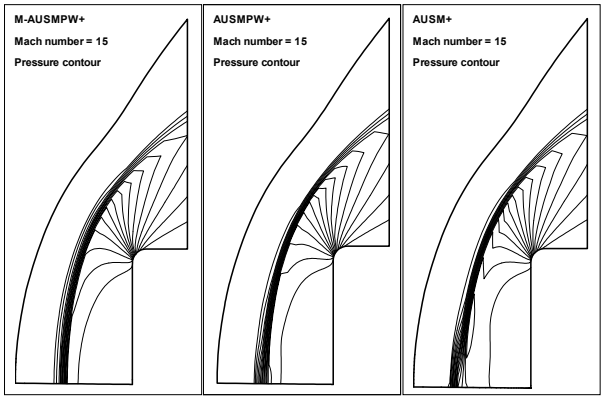

Fig. 8. Comparison of pressure contours of each scheme.

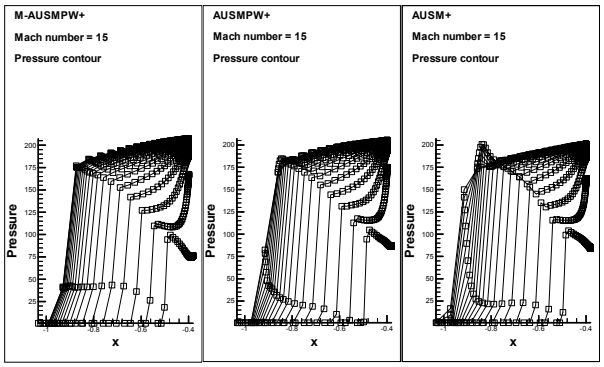

Fig. 9. Comparison of pressure distributions along the stagnation line.

Figure 8 and 9 show shock-capturing characteristic of each scheme in multi-dimensional problems and are the case that a sonic transition position and a cell-interface are located like Fig. 1(a). As shown in Fig. 1(a), AUSM+ and AUSMPW+ show oscillations. Moreover, the results of AUSM+ and AUSMPW+ cannot be converged because of oscillations. In contrast, as in one-dimensional results, M-AUSMPW does not show any numerical oscillations and it always maintains the monotonic characteristic. Independent to grid systems, M-AUSMPW+ can capture shock without oscillations.

7 Conclusions

Numerical oscillations in shocks, which is one of disadvantages of AUSM-type schemes, was analyzed and solutions for the removal of them are provided. AUSM+ which has the advection property cannot represent the physical phenomena accurately in subsonic or transonic flows. This disagreement between the advection property and physical phenomena directly leads to numerical oscillations. The inaccurate representation of physical phenomena induces excessive or insufficient fluxes and eventually shows oscillatory behavior. In order to settle this disadvantage, scheme should calculate accurate fluxes behind a shock discontinuity with right consideration of physical phenomena. M-AUSMPW+ is developed to remove oscillations completely in considering physical phenomena accurately as possible and whether a cell-interface of shock region is in subsonic or supersonic region. Independent to a sonic transition position, M-AUSMPW+ can capture shock accurately with the monotonic characteristic.

References

[1] Liou M S, and Steffen C J Jr.. A new flux splitting scheme. *J. of Computational Physics*, Vol. 107, pp 23-39, 1993.

[2] Liou M S. A sequel to AUSM: AUSM+. *J. of Computational Physics*, Vol. 129, pp 364-382, 1996.

[3] Kim K-H, Lee J-H and Rho O-H. An improvement of AUSM schemes by introducing the pressure-based weight functions. *Computers & Fluids*, Vol. 27, No. 3, pp 311-346, 1998.

[4] Kim K-H, Kim C and Rho O-H. Methods for the accurate computations of hypersonic flows, part I: AUSMPW+ scheme. *J. Computational Physics*, Vol. 174, pp 38-80, 2001.

[5] Kim K-H, Kim C and Rho O-H. Methods for the accurate computations of hypersonic flows, part II:

shock-aligned grid technique. *J. Computational Physics*, Vol. 174, pp 81-119, 2001.

[6] van Leer B. Flux-vector Splitting for the Euler Equation. *Lecture Notes in physics*, Vol. 170, pp 507-512, 1982.

[7] Sweby P K. High Resolution TVD Schemes Using Flux Limiters. *Lectures in Applied Mathematics*, Vol. 22, pp 289-309, 1985.

[8] Hirsh C. *Numerical Computation of Internal and External Flows*. Vol. 1,2, John Wiley & Sons, 1990.